An Alternative Approach of UASB Dynamic Modeling

Apostolos Vlyssides, Elli Maria Barampouti, and Sofia Mai
School of Chemical Engineering, National Technical University of Athens, Zografou 15700, Greece

DOI 10.1002/aic.11342
Published online October 25, 2007 in Wiley InterScience (www.interscience.wiley.com).

A mathematical model was developed and validated to simulate the dynamic behavior of a UASB reactor. This model took into consideration all the biological and physicochemical reactions. Seven microbial populations were selected using Monod kinetics where inhibition terms were added. The overall biological reactions were determined by first evaluating the reactions for energy and synthesis separately and then adding them together. For each differential time interval, the biomass produced was estimated from the stoichiometry of these reactions. The feasibility of each reaction was determined by thermodynamic calculations. A thermodynamic solution was suggested for the microorganisms that are able to follow more than one catabolic routes and produce several products in spite of the fact that they consume just one substrate. All the reactions that may be performed were realized according to the relative percentage of their free energies. The validation of the model was based on a set of dynamical experiments designed to cover a wide spectrum of operating conditions that are likely to take place in the practical operation of a UASB plant. The model can be a useful tool for the prediction of process performance in transient conditions, even in failure, and can be used to assist in the operation of biogas plants. © 2007 American Institute of Chemical Engineers *AIChE J,* 53: 3269–3276, 2007

Keywords: anaerobic digestion, dynamic model, thermodynamic data, biological reactions, physicochemical reactions

Introduction

In the past 20 years, upflow anaerobic sludge blanket (UASB) technology was developed for wastewater treatment.[1–6] The UASB reactor is considered desirable in high-strength organic wastewater treatment because of its high biomass concentration and rich microbial diversity.[5,7–10]

The anaerobic treatment plants, although used frequently at the industrial scale, they are known to become easily unstable under some circumstances, such as variations of the process operating conditions. Nevertheless, this drawback can be overcome by associating a monitoring procedure with a decision support system that allows the enhancement of the stable performance of the online wastewater treatment operation via a feedback control loop.[11–15] Therefore, a reliable dynamic model of the process is required for the design of such monitoring and control algorithms.

The dynamic modeling of anaerobic digestion has been an active research area during the last three decades. A dynamic model can be used for different purposes. One objective can be the numerical simulation of the process behavior; for example, for predicting its dynamical behavior or for identifying and understanding better the major mechanisms driving its dynamics. Another objective is the design of monitoring and control algorithms.[15] The aim of this article was the development of a UASB dynamic model that serves both objectives.

The article is organized as follows. The first section briefly describes the UASB reactor, the measurement devices and the considered methods. The modeling assumptions are then intro-

This article contains supplementary material available via the Internet at http://www.interscience.wiley.com/jpages/0001-1541/suppmat.

Correspondence concerning this article should be addressed to A. Vlyssides at avlys@tee.gr.

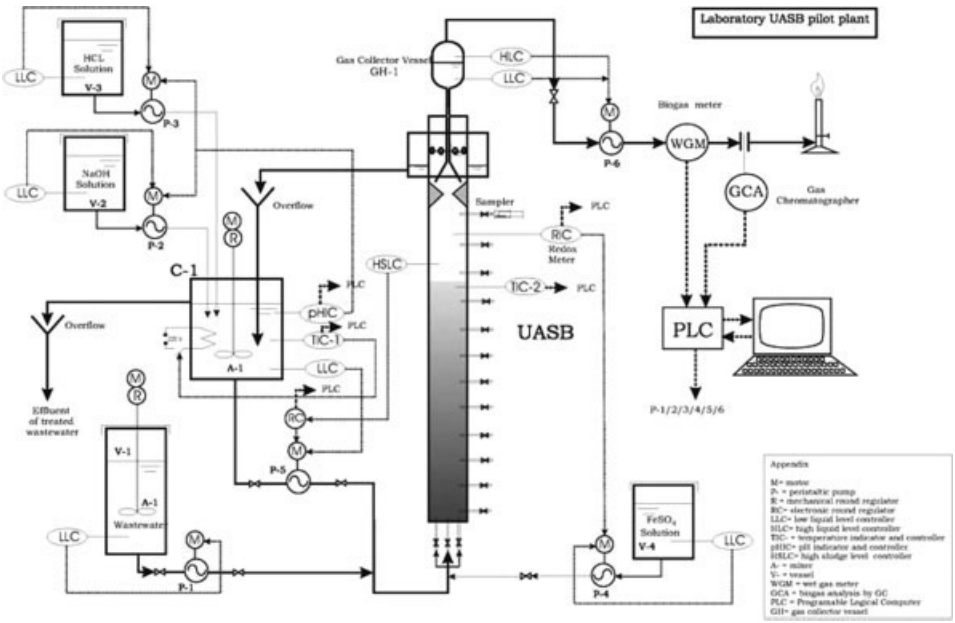

Figure 1. Laboratory scale UASB reactor.

duced in a second section. Then a description of the basic elements of the model (reaction network, chemical equilibria, hydrodynamics) is given. From these considerations, a mass-balance-based model consisting of a set of differential equations is derived. The kinetic parameters of the model are estimated using a first set of experimental data. Then the model is validated using another set of experimental data.

Materials and Methods

Composition of feed

Synthetic milk wastewater used in this study was prepared by diluting fat-free fresh milk. This synthetic milk wastewater ensured the presence of various micronutrients in contrast to most chemostatic feeds. Furthermore, this substrate could simulate dairy wastewater. The COD of this wastewater ranged from 2500 to 12,500 mg L^{-1}. The total nitrogen, total phosphorous and total sulphur of the wastewater ranged from 125 to 625 mg L^{-1}, 20 to 100 mg L^{-1}, and 14 to 71 mg L^{-1} respectively. pH varied between 6.5 and 7.0.

Reactor operating conditions

A Plexiglas laboratory-scale UASB reactor (Figure 1) with a volume of 20 L, was operated at 35°C. Hydraulic retention time was 20 h. The COD load was increased from 2.5 g COD L^{-1} d^{-1} to 12.5 g COD L^{-1} d^{-1} by a step of 2.5 g COD L^{-1} d^{-1} every 15 days.

During the reactor's operation, gas production and composition, COD and total sulphur concentrations in the influent and effluent were measured daily. Concentrations of bicarbonate alkalinity (ALK) and volatile fatty acids (VFA) were determined in the sludge bed. Sludge samples from all the sampling ports of the sludge bed of the reactors were collected for the determination of their density, total suspended and volatile solids content and settling characteristics. All analysis for pollution parameters were conducted in accordance with the standard methods.[16] All chemicals were of analytical or biological grade and purchased from E. Merck AG. The concentration and composition of VFA was analyzed by gas chromatography (HP Agilent 5890) using a flame ionization detector (FID) and a packed column suitable for VFA analysis. The produced gas was recorded by a wet gas meter (Ritter Gas meter Drum type TG01) and gas composition was analyzed by gas chromatography (HP Agilent 5890) using a thermal conductivity detector (TCD) and a packed column suitable for biogas. Argon was used as the carrier gas with flow rate of 30 mL min^{-1}.

Modeling and Theoretical Aspects

Model assumptions

The model included four biochemical (cellular) processes (acidogenesis, acetogenesis, methanogenesis, and sulphate reduction) and an extracellular process (hydrolysis). The hydrolysis rate followed first order kinetics.[17] The bacterial populations were assumed to be divided into seven main groups of homogeneous characteristics[18,19] (Figure 2):

(1) Fermentative bacteria FB, bacteria that decompose complex organic substrate into organic acids and then the latter into volatile fatty acids and carbon dioxide,

(2) Syntrophic bacteria 1 SB1, bacteria that convert propionic acid into acetic acid,

(3) Syntrophic bacteria 2 SB2, bacteria that convert butyric acid into acetic acid,

(4) Homoacetogenic bacteria HAB, bacteria that from hydrogen and carbon dioxide produce acetic acid,

(5) Acetophilic methanogenic bacteria AMB, bacteria that convert acetic acid into methane,

(6) Methanogenic bacteria MB, bacteria that convert hydrogen and carbon dioxide into methane,

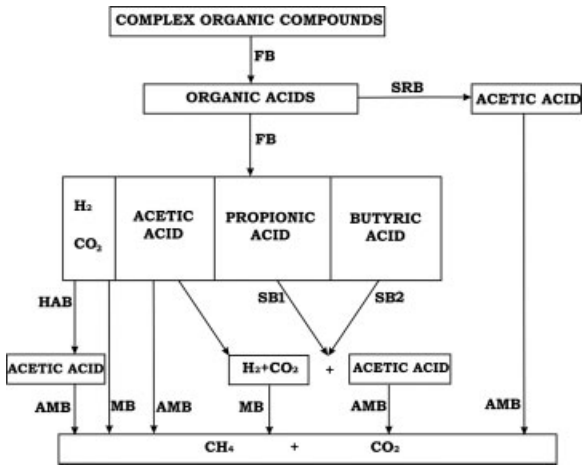

Figure 2. Microbial populations and respective reactions.

(7) Sulfate reducing bacteria SRB, bacteria that reduce sulfate ions to sulfide using organic acids as electron donor as well as carbon source.

Carbon (C) was chosen to be the chemical component base unit in mass basis. Molar basis was used for components with no carbon such as sulfur and hydrogen.

Kinetics

The substrate uptake rates of all microbial groups were considered to follow a Monod-type kinetics.

The following mechanisms of inhibition in biological processes were considered[17,20]:

(1) Noncompetitive
(2) Uncompetitive
(3) Competitive
(4) pH inhibition

These four types of inhibition were adjusted to the uninhibited Monod-type kinetics as follows:

1. $K = \dfrac{K_{\max} \times \text{Sub}}{K_S + \text{Sub}} \times \dfrac{K_I}{K_I + I}$

2. $K = \dfrac{K_{\max} \times \text{Sub}}{K_S + \text{Sub} \times \left(1 + \dfrac{K_I}{I}\right)}$

3. $K = \dfrac{K_{\max} \times \text{Sub}}{K_S \times \left(1 + \dfrac{I}{K_I}\right) + \text{Sub}}$

4. $K = \dfrac{K_{\max} \times \text{Sub}}{K_S + \text{Sub}} \times \dfrac{1 + 2 \times 10^{0.5 \cdot (\text{pH}_{LL} - \text{pH}_{UL})}}{1 + 10^{(\text{pH} - \text{pH}_{UL})} + 10^{(\text{pH}_{LL} - \text{pH})}}$

where:

Sub is the concentration of substrate for process
I is the concentration of inhibitor
pH_{UL} and pH_{LL} are upper and lower limits where the group of organisms is 50% inhibited respectively.

In the model that was constructed, inhibition of unionized fatty acids, ammonia, dissolved carbon dioxide, molar hydrogen, solution ionic strength, hydrogen sulfide, and pH needed to be accounted for. Taking into consideration the literature and the bacterial reactions, the following matrix was formed (Table 1). This table presents the type of inhibition that was assumed for each microorganism. Table 2 presents the values of inhibition coefficients taken from literature for similar anaerobic processes and substrates.

Evaluation of stoichiometric coefficients of overall biological reactions

Reaction equations with proper stoichiometric coefficients can be devised for overall biological reactions by first evaluating the reactions for energy and synthesis separately and then adding them together (Supplementary Material). Heterotrophic and chemosynthetic autotrophic microorganisms obtain energy for growth by mediating oxidation–reduction reactions. Such reactions involve a flow of electrons from electron donors to electron acceptors. For the synthesis reactions, the chemical formula of bacterial cells was assumed to be $C_5H_7O_2N$.[17]

For each i reaction, E_i represents the electron equivalents of the electron donor converted for energy per electron equivalent of cells synthesized. Thus, each overall biological reaction derives from the addition of the energy reaction and the synthesis reaction divided by E_i. The values of E_i can be approximated from considerations of the energy released by the energy reactions, the energy required for synthesis, and the efficiency by which energy is transferred in these reactions.

McCarty (1971)[29] presented the following equation for the estimation of E_i.

$$E_i = -\frac{\Delta G_{pi}/e^m + \Delta G_{ni}/e + \Delta G_{ci}}{e\Delta G_i} \quad (1)$$

The terms in the numerator represent the quantity of energy required to synthesize an electron equivalent of cells. The term ΔG_{pi} represents the quantity of energy required to convert the carbon source used for synthesis of cells mediating i reaction into an intermediate (assumed to be pyruvate for energy calculations). This is obtained by subtracting ΔG^o for the pyruvate half reaction ($=-8.54$ kcal eq^{-1}) from ΔG^o for the half-reaction involving the cell carbon source. ΔG_{ci} represents the energy for conversion of intermediate into cells and was estimated to be equal to 7.5 kcal eq^{-1}.[29]

ΔG_{ni} represents the energy required to reduce the nitrogen source used for cell synthesis into ammonia. ΔG_{ni} equals zero if the nitrogen source is ammonia, the usual nitrogen source in methane fermentations.

Table 1. Type of Inhibition* for Each Microorganism and Inhibitor

	VFA	NH_3	CO_{2aq}	H_2	Ionic strength	H_2S_{aq}	pH
FB	3	1	3	3	1	1	4
SB1	0	1	3	1	1	1	4
SB2	0	1	3	1	1	1	4
HAB	3	1	2	0	1	1	4
MB	3	1	2	0	1	1	4
AMB	3	1	3	1	1	1	4
SRB	0	1	3	2	1	3	4

*0 = No inhibition, 1 = Noncompetitive inhibition, 2 = Uncompetitive inhibition, 3 = Competitive inhibition, 4 = pH inhibition.

Table 2. Inhibition Coefficients for Each Microorganism and Inhibitor

	VFA (gC L^{-1})	NH_3 (mol L^{-1})	CO_{2aq} (gC L^{-1})	H_2 (mol L^{-1})	Ionic strength	H_2S_{aq} (mol L^{-1})
FB	0.00005[17,21]	0.1[22]	0.0005[23]	0.001[17,21]	*	0.0008[24]
SB1	–	0.002[17,21]	1[23]	0.01[17,21]	10^{25}	0.002[24]
SB2	–	0.004[22]	1[23]	0.01[17,26]	10^{25}	0.004[24]
HAB	1[15]	0.005[24]	0.001[23]	–	10^{25}	0.005[24]
MB	0.7[15]	0.0006[22]	*	–	*	0.006[24]
AMB	0.6[15]	0.00068[17,21]	0.03[23]	*	*	0.006[24]
SRB	–	0.001[27]	1[27]	5×10^{-10}[27]	10^{27}	0.0068[28]

*The inhibition coefficients estimated through experimental data.

The denominator of Eq. 1 represents the energy released and available for the synthesis reaction per electron equivalent of change for the energy reaction. The value ΔG_i, is a function of the activities of reactants and products and is determined by use of the following equation:

$$\Delta G_i = \Delta G_i^\circ + RT \sum_{j=1}^{m} u_j \ln \alpha_j \quad (2)$$

where ΔG_i° is the standard free energy for i reaction

u_j are the stoichiometric coefficients of i reaction

a_j is the activity of component A_j in i reaction

The activity for nongaseous components is approximated by their molar concentration and for gaseous components by their partial pressure.

The value of e represents the efficiency of energy conversion, and for autotrophic and heterotrophic bacteria growing under suitable environmental conditions generally varies from about 0.4 to 0.8 with an average of about 0.6. The value for m is $+1$ for $\Delta G_{pi} > 0$ and -1 for $\Delta G_{pi} < 0$.[29]

According to the theory mentioned above, the overall biological reactions were determined and incorporated in the model. For each differential time interval, the biomass produced was estimated from the stoichiometry of these reactions, in contrast to the conventional anaerobic models where a constant Y (maximum cell yield coefficient) is used. Furthermore, the feasibility of each reaction was determined by thermodynamic calculations, ΔG_i.

From Figure 2, it is obvious that the fermentative bacteria, while consuming the same substrate, may produce either acetic acid, or propionic acid, or butyric acid, or hydrogen and carbon dioxide. In other words, the fermentative bacteria perform simultaneously four different biological reactions. In anaerobic digestion, this phenomenon is very common. Many bacterial populations are able to follow more than one different catabolic routes and produce several products in spite of the fact that they consume just one substrate. For this reason, during mathematical modeling of anaerobic digestion, the issue of choice of the possible routes is set. In this model, for these microorganisms, a thermodynamic solution is suggested. All the reactions that may be performed are realized according to the relative percentage of their free energies.

In particular, the fermentative bacteria are divided in four subgroups according to the four possible reactions. The percentage of fermentative bacteria of each subgroup is calculated for each differential time interval from the relative percentage of the free energies of the four possible reactions.

Physicochemical processes

The physicochemical system can be defined as nonbiologically mediated processes that commonly occur in anaerobic reactors. There are three broad types listed below according to the relative kinetic rates:

(1) Liquid–liquid processes (i.e. ion association/dissociation: rapid)

(2) Liquid–gas processes (i.e. liquid-gas transfer: rapid/medium)

(3) Liquid–solid processes (i.e. precipitation/solubilization: medium/slow)

In the literature,[17,24] only the first two process types have been commonly addressed in anaerobic models, whereas this was not the case for this model.

Liquid–liquid processes

Volatile Fatty Acids. The volatile fatty acids that were taken into account in this model were acetic, propionic, and butyric acid. For each species, the total concentration of VFA is composed of ions VFA^- and unionized VFA_{mol}. The corresponding dissociation constant is equal to:

$$K_a = \frac{H^+ \times VFA^-}{VFA_{mol}} \quad (3)$$

The numerical value of K_a in the considered pH range is 1.76×10^{-5} mol L^{-1} for acetic acid, 1.34×10^{-5} for propionic acid and 1.54×10^{-5} for butyric acid.[30]

Ammonia. The total concentration of ammonia NH_3 is composed of ions NH_4^+ and unionized ammonia NH_{3mol}. The corresponding dissociation constant is equal to:

$$K_b = \frac{OH^- \times NH_4^+}{NH_{3mol}} \quad (4)$$

The numerical value of K_b is 1.79×10^{-5} mol L^{-1}.[30]

Inorganic Carbon. The chemical reactions involving the inorganic carbon are mainly composed of dissolved carbon dioxide (CO_{2aq}), bicarbonate (HCO_3^-), carbonic acid (H_2CO_3) and carbonate (CO_3^{2-}) in line with Bernard et al. (2001). The total inorganic carbon C_{in} is equal to:

$$C_{in} = CO_{2aq} + H_2CO_3 + HCO_3^- + CO_3^{2-} \quad (5)$$

These species are in equilibrium according to the following reactions[30]:

$$CO_{2aq} + H_2O \rightarrow H_2CO_3 \quad K_1 = \frac{H_2CO_3}{CO_{2aq}} = 1.3 \times 10^{-3} \quad (6)$$

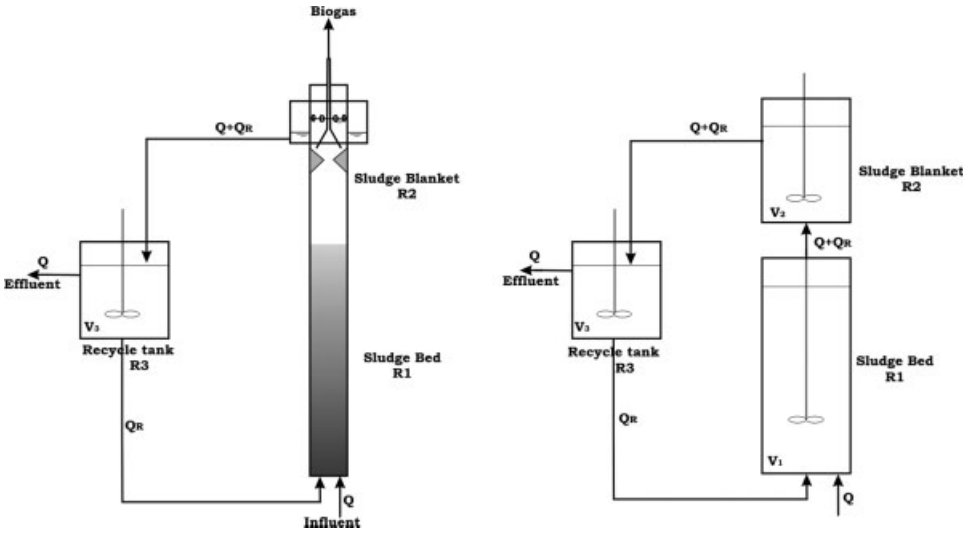

Figure 3. Flow rate profile.

$$H_2CO_3 \rightarrow H^+ + HCO_3^- \quad K_2 = \frac{H^+ \times HCO_3^-}{H_2CO_3} = 2 \times 10^{-4} \tag{7}$$

$$HCO_3^- \rightarrow H^+ + CO_3^{2-} \quad K_3 = \frac{H^+ \times {CO_3}^{2-}}{HCO_3^-} = 4.69 \times 10^{-11} \tag{8}$$

Total Sulfur. The chemical reactions involving the sulphur are mainly composed of: dissolved H_2S (H_2S_{aq}), sulfide ions (S^{2-}), hydrogen sulfide ions (HS^-) and sulfate ions (SO_4^{2-}). The total inorganic sulfur (TS) is equal to:

$$TS = H_2S_{aq} + S^{2-} + HS^- + SO_4^{2-} \tag{9}$$

These species are in equilibrium according to the following reactions.[30]:

$$H^+ + S^{2-} \rightarrow HS^- \quad K_{1,S} = \frac{HS^-}{H^+ \times S^{2-}} = 8.33 \times 10^{12} \tag{10}$$

$$H^+ + HS^- \rightarrow H_2S_{aq} \quad K_{2,S} = \frac{H_2S_{aq}}{H^+ \times HS^-} = 10^7 \tag{11}$$

pH Determination. For the pH determination, the central equation is the charge balance of ionic species (Eq. 12) in the reactor which is solved simultaneously with the mass balances.[24,31]

$$HCO_3^- + 2 \cdot CO_3^{2-} + HS^- + 2 \cdot S^{2-} + 2 \cdot SO_4^{2-} + VFA^- + OH^- = NH_4^+ + H^+ + Z^+ \tag{12}$$

where Z^+ is the concentration of all cations apart from H^+ and NH_4^+.

Liquid–gas transfer

The following four main gas components are considered significant as intermediates and as having a strong effect on biological processes:

CH_4–relatively low solubility
CO_2–relatively high solubility
H_2S–high solubility
H_2–high solubility

Because of the very low solubility of methane, the concentration of dissolved methane is neglected and the produced methane is assumed to go directly out of the fermenter with a molar flow rate proportional to the reaction rate of methanogenesis.

The molar flow rate (q_C) for CO_2, H_2S and H_2 can be computed using Henry's law:

$$q_{C,i} = k_L a_i \cdot (C_{aq,i} - K_{H,i} \cdot pi) \tag{13}$$

Liquid–solid processes

Solids precipitation is the complexing of cations and anions in neutral inorganic solid form. Potentially important solid precipitants in anaerobic digesters include calcium carbonate, calcium hydroxide, calcium phosphate, magnesium carbonate and metal sulfide precipitates. The most important forms of precipitates are calcium carbonate and calcium hydroxide and thus they were chosen to be addressed in the present article.[32,33]

$$Ca^{2+} + CO_3^{2-} \rightarrow CaCO_{3s} \quad K_{sp} = 10^8 \tag{14}$$

$$Ca^{2+} + 2OH^- \rightarrow Ca(OH)_{2s} \quad K_{sp} = 10^{3.75} \tag{15}$$

The liquid–solid equilibriums are not assumed instant. Thus, a transfer rate (q_s) from the liquid to the solid phase was considered[34]:

$$q_{s,i} = k_L s_i \cdot (C_{aq,i} - C_{aq,th,i}) \tag{16}$$

Hydrodynamics of the fermenter

In studies on the fluid-flow pattern in upflow reactors, it was found that both the sludge bed and the sludge blanket

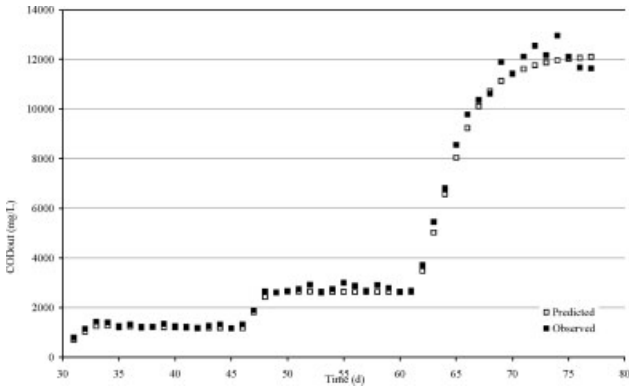

Figure 4. COD concentrations in the effluent (measured and predicted from the model) for loading rates 7.5–12.5 g COD L^{-1} d^{-1}.

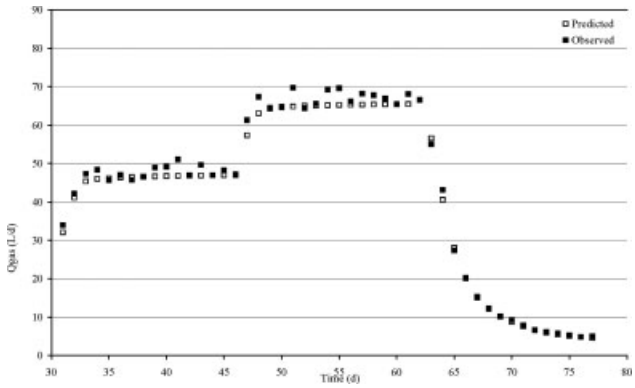

Figure 5. Daily biogas production (measured and predicted from the model) for loading rates 7.5–12.5 g COD L^{-1} d^{-1}.

can be described as separate, well-mixed flow regions. Consequently, in the description of the fluid flow pattern, two ideal mixers were taken for these two areas.[15,35–39] The recirculation tank was considered as the third ideal mixer (Figure 3).

Results

Model implementation

A number of different modules describing the rate of biological reactions, the equilibrium solution chemistry, the liquid-gas and liquid-solid mass transfer were constructed. Combined, these resulted in a system of differential algebraic equations. Apart from Henry's Law constants, dissociation constants, molecular weights and COD values, which are easily calculated or obtained from standard chemistry textbooks, the model has a large number of parameters for the calculation of the rates of the biological reactions. All the parameters required were obtained from a survey of published anaerobic kinetic constants except for the following inhibition constants:

– CO_2 for methanogenic bacteria
– H_2 for acetophilic methanogenic bacteria
– Ionic strength for fermentative, methanogenic and acetophilic methanogenic bacteria

First-order integration in time with a variable time step was performed in a sequence of calculations/steps by a computer program. The program was written in Visual Basic in a generalized form, where a variable number of steps, organisms, components and kinetic models with associated data as well as substrate and inoculum specifications could be specified through input data. The program allowed interactive user control of external parameters such as hydraulic loading, temperature and substrate composition.

The experimental record data that derived from the implementation of COD loads 2.5 g COD L^{-1} d^{-1} and 5 g COD L^{-1} d^{-1} was used for the parameters estimation. The unknown inhibition constants were estimated aiming the optimum prediction of biogas production rate, COD concentration in the effluent, CH_4, CO_2, H_2S, H_2 content in biogas, composition and concentration of volatile fatty acids.

Simulation results

The model has been successfully used to simulate the operation of the reactor in an unknown data range of higher loading rates from 7.5 to 12.5 g COD L^{-1} d^{-1}. For loading rates up to 10 g COD L^{-1} d^{-1}, the performance of the reactor was satisfactory with COD digestion rate higher than 80%. However, when the COD loading rate was increased, the system was led to failure given the high effluent COD concentrations and the sudden drop of biogas production (Figures 4 and 5).

The response of the model was compared to the experimental data. Plots of actual and simulated COD concentrations in the effluent and biogas production are shown in Figures 4 and 5. The predicted values are in good agreement with the experimental values. Apart from the variables presented in Figures 4 and 5, the model prediction fitted well to:

– pH values in the sludge bed (Figure 6)
– biogas composition (Figure 7)
– composition and concentration of volatile fatty acids (Figures 8 and 9)

Figures 4–9 cannot give sufficient information for the adequacy of the model that was constructed. To check the model, goodness of fit X^2 test was conducted according to

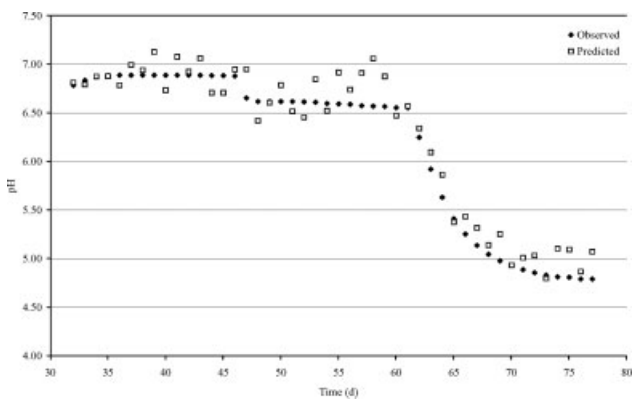

Figure 6. pH in the sludge bed (measured and predicted from the model) for loading rates 7.5–12.5 g COD L^{-1} d^{-1}.

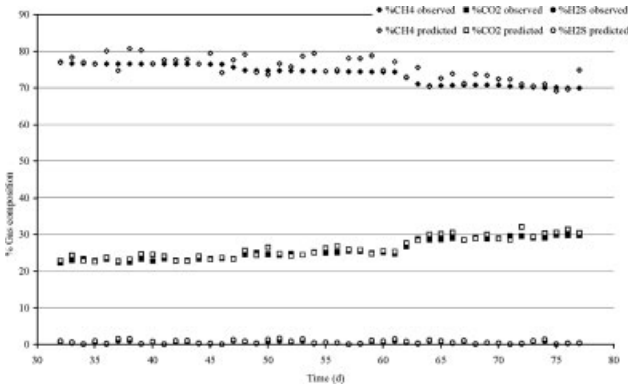

Figure 7. Biogas composition (measured and predicted from the model) for loading rates 7.5–12.5 g COD L^{-1} d^{-1}.

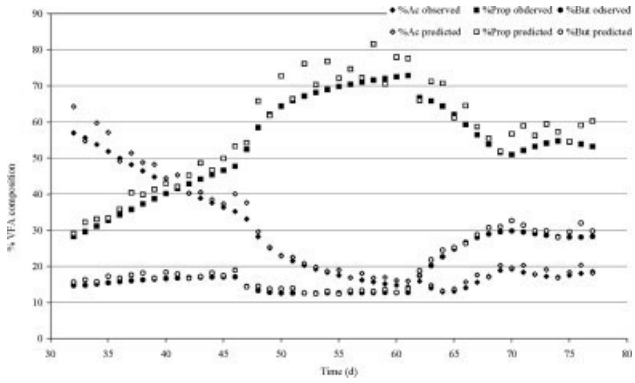

Figure 9. Composition of volatile fatty acids (measured and predicted from the model) for loading rates 7.5–12.5 g COD L^{-1} d^{-1}.

Parratt (1961).[40] By this test it was examined how well the developed dynamic model fitted a set of observations. It was performed to test whether the observed frequencies differ significantly from the expected frequencies. The chi-square statistic is a sum of differences between observed and expected outcome frequencies, each squared and divided by the expectation. The resulting values were compared with chi-square distribution and the goodness of fit was determined. For the COD concentrations in the effluent, the probability was estimated and was equal to 0.835. For given degrees of freedom and significance level, the model can be considered very satisfactory. The respective value for biogas production was 0.871, so the model also predicted well the biogas production. Thus, the results of X^2 test revealed that the model can be a satisfactory prediction tool.

Conclusions

A mathematical model able to simulate the dynamic behavior of an anaerobic UASB digester was developed and validated. In this model all the biological and physicochemical reactions were accounted for. The innovative points in the model structure are:

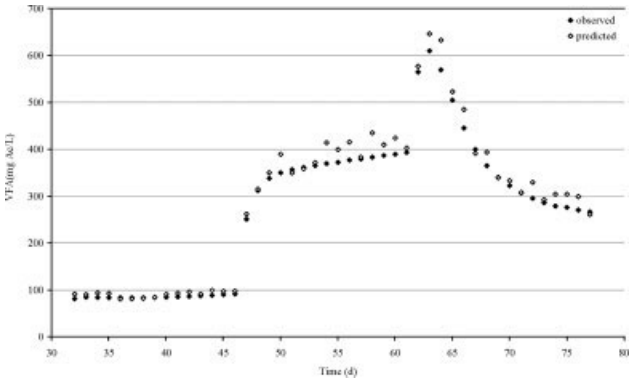

Figure 8. Total concentration of volatile fatty acids (measured and predicted from the model) for loading rates 7.5–12.5 g COD L^{-1} d^{-1}.

– the thermodynamic solution for the microorganisms that are able to follow more than one catabolic routes and produce several products in spite of the fact that they consume just one substrate.

– The fact that the biomass produced was estimated from the stoichiometry of energy and synthesis reactions, in contrast to the conventional anaerobic models where a constant Y (maximum cell yield coefficient) is used.

– The feasibility of each reaction was determined for each differential time interval by thermodynamic calculations, ΔG_i.

First-order integration in time with a variable time step was performed in a sequence of calculations/steps by a computer program. Experiments were designed covering a wide range of experimental conditions in order to develop and validate the model. This diversity was obtained via various organic loading rates given various influent COD concentrations.

During the model's simulation, it proved to be efficient in dynamical conditions, since not only the organic loading rates were gradually increased, but the sludge bed characteristics never achieve steady state conditions. Another important point is that this model predicted the system's failure in high organic load, something that the conventional mathematical models hardly achieve.

Conclusively, the model can be a useful tool for the prediction of process performance in the future and can be used to assist in the operation of biogas plants.

Acknowledgments

This work was done under the operational Program for Educational and Vocational Training II (EPEAEK II) and particularly the Program HRAKLEITOS. The project is co - funded by the European Social Fund (75%) and National Resources (25%).

Notation

$C_{aq,i}$ = concentration of soluble i component, mol L^{-1}
$C_{aq,th,i}$ = theoretical maximum concentration of i soluble component, mol L^{-1}
C_{in} = concentration of inorganic carbon, gC L^{-1}
CO_2 = concentration of CO_2 gas, gC L^{-1}
CO_{2aq} = concentration of soluble CO_2, gC L^{-1}
CO_3^{2-} = concentration of carbonate ions, gC L^{-1}
H^+ = concentration of hydrogen ions, mol L^{-1}
H_2 = concentration of hydrogen, mol L^{-1}

H_2CO_3 = concentration of carbonic acid, gC L^{-1}
H_2S = concentration of hydrogen sulfide gas, mol L^{-1}
H_2S_{aq} = concentration of soluble hydrogen sulfide, mol L^{-1}
HCO_3^- = concentration of bicarbonate ions, gC L^{-1}
HS^- = concentration of hydrogen sulfur ions, mol L^{-1}
$K_{H,i}$ = Henry's law constant for i gas, mol atm^{-1} L^{-1}
$k_La_{,i}$ = gas–liquid transfer coefficient for i gas, d^{-1}
$k_{LS,i}$ = solid–liquid transfer coefficient for i solid precipitate, d^{-1}
K_{max,X_i} = Monod maximum specific growth rate, d^{-1}
K_{X_i} = specific growth rate, d^{-1}
NH_3 = concentration of ammonia, gN L^{-1}
NH_{3mol} = concentration of nonassociated ammonia, gN L^{-1}
NH_4^+ = concentration of ammonia ions, gN L^{-1}
OH^- = concentration of hydroxyl ions, mol L^{-1}
p_i = partial pressure of i gas
Q = influent flow rate, L d^{-1}
$q_{c,i}$ = molar flow rate of i gas, mol L^{-1} d^{-1}
Q_r = recycle flow rate, L d^{-1}
$q_{s,i}$ = flow rate of i solid precipitate, mol L^{-1} d^{-1}
S^{-2} = concentration of sulfur ions, mol L^{-1}
SO_4^{2-} = concentration of sulfate ions, mol L^{-1}
TS = concentration of total sulfur, mol L^{-1}
VFA = concentration of volatile fatty acids, gC L^{-1}
VFA^- = concentration of associated volatile fatty acids, gC L^{-1}
VFA_{mol} = concentration of nonassociated volatile fatty acids, gC L^{-1}
Y_{X_i} = yield of biomass, gC gC^{-1}

Literature Cited

1. Lettinga G, van Velsen AFM, Hobma SW, de Zeeuw W, Klapwijk A. Use of the upflow sludge blanket (USB) reactor concept for biological wastewater treatment, specially for anaerobic treatment. *Biotechnol Bioeng*. 1980;22:699–734.
2. Lettinga G, Hulshoff Pol LW, Koster IW, Wiegant WM, Zeeuw WJ, de Rinzema A, Grin PC, Roersma RE, Hobma SW. High-rate anaerobic wastewater treatment using the UASB reactor under a wide range of temperature conditions. *Biotechnol Genet Eng*. 1984;2:253–284.
3. Alphenaar PA, Visser A, Lettinga G. The effect of liquid upflow velocity and hydraulic retention time on granulation in UASB reactors treating wastewater with a high-sulphate content. *Bioresource Technol*. 1993;43:249–258.
4. Fang HHP, Chui HK. Maximum COD loading capacity in UASB reactors at 37°C. *J Environ Eng ASCE*. 1993;119:103–119.
5. Schmidt JE, Ahring BK. Granular sludge formation in upflow anaerobic sludge blanket (UASB) reactors. *Biotechnol Bioeng*. 1996;49: 229–246.
6. Tay JH, Yan YG. Influence of substrate concentration on microbial selection and granulation during start-up of upflow anaerobic sludge blanket reactors. *Water Environ Res*. 1996;68:1140–1150.
7. Hulshoff Pol LW. *The Phenomenon of Granulation of Anaerobic Sludge*. PhD Thesis, Wageningen Agricultural University, Wageningen, 1989.
8. Lettinga G, Man AD, ver der Last ARM, Wiegant W, van Knippenberg K, Frijns J, van Buuren JCL. Anaerobic treatment of domestic sewage and wastewater. *Water Sci Technol*. 1993;27:67–73.
9. Fang HHP, Chui HK, Li YY, Chen T. Performance and granule characteristics of UASB process treating wastewater with hydrolyzed proteins. *Water Sci Technol*. 1994;30:55–63.
10. Ghangrekar MM, Asolekar SR, Joshi SG. Characteristics of sludge developed under different loading conditions during UASB reactor start-up and granulation. *Water Res*. 2005;39:1123–1133.
11. Fripiat J, Bol T, Binot R, Nyns E. *A Strategy for the Evaluation of Methane Production from Different Types of Substrate Biomass*. Exeter: Roger Bowskill, 1984.
12. Dochain D, Perrier M, Pauss A. Adaptive control of the hydrogen concentration in anaerobic digestion. *Ind Eng Chem Res*. 1991;30:129–136.
13. Perrier M, Dochain D. Evaluation of control strategies for anaerobic digestion processes. *Int J Adapt Control Sign Proc*. 1993;7:309–321.
14. Steyer JP, Buffiere P, Rolland D, Moletta R. Advanced control of anaerobic digestion processes through disturbances monitoring. *Water Res*. 1999;33:2059–2068.
15. Bernard O, Hadj-Sadok Z, Dochain D, Genovesi A, Steyer JP. Dynamical Model development and parameter identification for an anaerobic wastewater treatment process. *Biotechnol Bioeng*. 2001;75:424–438.
16. APHA. *Standard Methods for the Examination of Water and Wastewater*. Washington, DC: American Public Health Association, 1985.
17. IWA Task Group for mathematical modelling of anaerobic digestion processes. Anaerobic Digestion Model No. 1 (ADM1). Scientific and Technical report No. 13. London: IWA, 2002.
18. Bruce AM, Kouzeli-Katsiri A, Newman PJ. *Anaerobic Digestion of Sewage Sludge and Organic Agricultural Wastes*. Athens: Comm. Eur. Communities, 1986.
19. Marchaim U. *Biogas Processes for Sustainable Development*. Rome: FAO, 1992.
20. Pavlostathis SG, Giraldo-Gomez E. Kinetics of anaerobic treatment: a critical review. *Crit Rev Env Control*. 1991;21:411–490.
21. Siegrist H, Vogt D, Garcia-Heras JL, Gujer W. Mathematical model for meso- and thermophilic anaerobic sewage sludge digestion. *Environ Sci Technol*. 2002;36:1113–1123.
22. Angelidaki I, Ellegaard L, Ahring BK. A comprehensive model of anaerobic bioconversion of complex substrates to biogas. *Biotechnol Bioeng*. 1999;63:363–372.
23. Knobel AN, Lewis AE. A mathematical model of a high sulphate wastewater anaerobic treatment system. *Water Res*. 2002;36:257–265.
24. Vavilin VA, Vasiliev VB, Rytov SV, Ponomarev AV. Modeling ammonia and hydrogen sulfide inhibition in anaerobic digestion. *Water Res*. 1995;29:827–835.
25. Bhatia D, Vieth WR, Venkatasubramanian K. Steady-state and transient behavior in microbial methanification: II. Mathematical modeling and verification. *Biotechnol Bioeng*. 1985;27:1199–1207.
26. Romli M, Keller J, Lee PL, Greenfield PF. Model prediction and verification of a two-stage high-rate anaerobic wastewater treatment system subjected to shock loads. *Process Saf Environ Protection*. 1995;73:151–154.
27. Tartakovsky B, Morel E, Steyer JP, Guiot SR. Application of a variable structure model in observation and control of an anaerobic digestor. *Biotechnol Progr*. 2002;18:898–903.
28. Kalyuzhnyi SV, Davlyatshina MA. Batch anaerobic digestion of glucose and its mathematical modeling. I. Kinetic investigations. *Bioresource Technol*. 1997;59:73–80.
29. McCarty PL. Energetics and kinetics of anaerobic treatment. *Adv Chem Ser*. 1971;105:91–107 (Anaerobic Biol. Treat. Process).
30. Butler JN. *Ionic Equilibrium: A Mathematical Approach*. Boston: Addison-Wesley, 1964.
31. Angelidaki I, Ellegaard L, Ahring BK. A mathematical model for dynamic simulation of anaerobic digestion of complex substrates: focusing on ammonia inhibition. *Biotechnol Bioeng*. 1993;42:159–166.
32. Keinath TM, Wanielista M. *Mathematical Modeling for Water Pollution Control Processes*. Michigan: Ann Arbor Science, 1975.
33. Van Langerak EPA, Beekmans MMH, Beun JJ, Hameleres HVM, Lettinga G. Influence of phosphate and iron on the extent of calcium carbonate precipitation during anaerobic digestion. *J Chem Technol Biotechnol*. 1999;74:1030–1036.
34. Vlyssides A, Barampouti EM, Mai S. Effect of ferrous ion on the biological activity in a UASB reactor: mathematical modeling and verification. *Biotechnol Bioeng*. 2007;96:853–861.
35. Buijs C, Heertjes PM, Van der Meer RR. Distribution and behavior of sludge in upflow reactors for anaerobic treatment of wastewater. *Biotechnol Bioeng*. 1982;24:1975–1989.
36. Van der Meer RR, Heertjes PM. Mathematical description of anaerobic treatment of wastewater in upflow reactors. *Biotechnol Bioeng*. 1983;25:2531–2556.
37. Bolle WL, Breugel J, Eybergen G, Kossen N, Zoetemeyer RJ. Modeling the liquid flow in up-flow anaerobic sludge blanket reactors. *Biotechnol Bioeng*. 1986;28:1615–1621.
38. Singhal A, Gomes J, Praveen VV, Ramachandran, KB, Axial dispersion model for upflow anaerobic sludge blanket reactors. *Biotechnol Progr*. 1998;14:645–648.
39. Ojha CSP, Singh RP. Flow distribution parameters in relation to flow resistance in an upflow anaerobic sludge blanket reactor system. *J Environ Eng*. 2002;128:196–200.
40. Parratt GL. *Probability and Experimental Errors in Science*. New York: Wiley, 1961.

Manuscript received Feb. 6, 2007, and revision received Aug. 28, 2007.